Feasibility of Accelerated 3D T1-Weighted MRI using Compressed-SENSE: Application to Quantitative Volume Measurement of Human Brain Structures

Uten Yarach (uten178@yahoo.co.th)
Chiang Mai University Faculty of Associated Medical Sciences https://orcid.org/0000-0002-5923-2864
Suwit Saekho
Chiang Mai University Faculty of Science
Kawin Setsompop
Stanford University Department of Radiology
Atita Suwannasak
Chiang Mai University Faculty of Associated Medical Sciences
Ratthaporn Boonsuth
Chiang Mai University Faculty of Associated Medical Sciences
Kittichai Wantanajittikul
Chiang Mai University Faculty of Associated Medical Sciences
Salita Angkurawaranon
Chiang Mai University Faculty of Medicine
Chaisiri Angkurawaranon
Chiang Mai University Faculty of Medicine
Prapatsorn Sangpin
Philips Healthcare

Research Article

Keywords: MRI, Parallel imaging, Compressed SENSE, 3D-T1 weighted, Subcortical structures, Brain volume measurement

Posted Date: February 5th, 2021

DOI: https://doi.org/10.21203/rs.3.rs-172465/v1

Abstract

Objective

Scan time reduction is crucial for volumetric acquisitions to improve workflow productivity and to reduce motion artifact during MRI procedure. We find out whether Compressed SENSE-4 (CS-4) can be pushed with 3D-turbo-field-echo T1-weighted (3D-TFE-T1W) sequence without compromising subcortical measurements on clinical 1.5T MRI.

Materials and methods

Thirty-three healthy volunteers (24 females, 9 males) underwent 1.5T MRI equipped with 12-channel coil. 3D-TFE-T1W for whole brain coverage was performed with different acceleration factors including SENSE-2, SENSE-4, CS-4. Freesurfer, FSL's FIRST, and volBrain packages were implemented for subcortical segmentations. All processed data were assessed using Wilcoxon signed-rank test. A *p-value* < 0.05 was considered statistically significant.

Results

In comparison with reference, signal-to-noise ratio (SNR) obtained by CS-4 slightly dropped, in which the maximum SNR drop was detected at Amygdala with value of 10.55%. However, such disadvantage did not affect volume measurements - there were no statically significant differences for all subcortical structures ($p < 0.05$). They were in strong correlation, in which Pearson's correlation coefficients were larger than 0.90. Moreover, the effect size scores are mostly in trivial to small ranges with values of 0.07–0.23.

Conclusion

CS-4 provided sufficient quality of 3D-TFE-T1W images for 1.5T MRI equipped with 12-channel receive coil. Subcortical volumes obtained from CS-4 images were consistent across different post-processing packages.

Introduction

The assessment of brain volume loss can represent a valid biomarker of clinical progression in neurodegenerative diseases (e.g., Alzheimer's and Parkinson's diseases) providing insights into the understanding of physiological and pathological mechanisms leading to brain atrophy [1–4]. Three dimension (3D) magnetic resonance imaging (MRI) has been increasingly popular and become a standard tool for investigating brain aging associated with multiple structural changes [5–9]. However, several minutes to acquire the necessary data,

particularly 3D high-resolution imaging sequences. Lengthy scan times are uncomfortable for patients and introduce the potential for motion [10] which causes artifacts in the images, thereby compromising the accuracies of clinical diagnosis, treatment planning, and quantitative analysis [11].

Over the last two decades, the advent of parallel imaging has changed the way MRI in clinical uses [12–14]. Parallel MRI (pMRI) is a robust way to accelerate data acquisition which allows a significant reduction in scan time by using the spatial information inherent in a multiple receiver coil array in combination with dedicated reconstruction algorithms. Its benefits include decreased motion artifact, reduced breath-hold time, shorter durations of diagnostic exams, and an increase in a number of series per exam [15–16]. Sensitivity encoding (SENSE) [12] and generalized autocalibrating partially parallel acquisitions (GRAPPA) [13] have been two parallel imaging methods widely used on clinical scanners. For the brain volume measurement MRI, 3D T1-weighted sequences (MPRAGE, IR-FSPGR, TFE) has been standard sequences and highly recommended by the Alzheimer's disease neuroimaging initiative (ADNI) [5] and the enhancing neuroimaging genetics through meta-analysis (ENIGMA) [7] consortiums, because it provides excellent gray-white mater contrast and high spatial resolution with whole brain coverage. Typically, this sequence takes about 9–10 minutes for non-accelerated MRI scan. Some studies reported that accelerated with factor of two and non-accelerated MRI scans yielded comparable results for brain volume measurement [17–20]. However, there is still a tremendous need to reduce scan time of these volumetric acquisitions to improve workflow productivity and to reduce the likelihood of motion during the scan. Unfortunately, higher than acceleration factor of two is likely not encouraged through SENSE and GRAPPA due to high g-factor noise amplification that increases proportionally to the increase of acceleration factor.

Within the past decade, another accelerated MRI technique has been developed so-called Compressed sensing [21–22]. It allows high quality images from undersampled k-space data by solving a constrained minimization problem using nonlinear optimization algorithm by enforcing the sparsity of images in a certain predefined sparsifying transform, such as the traditional 2D separable wavelet transform and total variation (TV). Various studies [23–25] have shown that offline Compressed sensing reconstructions outperform the conventional parallel imaging methods when regularization parameters are fine-tuned properly. Recently, Compressed sensing so-called Compressed-SENSE (CS) became a commercial product on clinical scanners with requires less actions from users for parameter fine-tuning. Application of CS on brain volume measurement was demonstrated recently, and found that CS with acceleration factor up to four had no major impact on image quality and morphometric measures [26–28]. However, these studies were performed on 3T MRI with 32-ch and 64-ch receive coils as well as only main components, such as gray matter, ventricles, and white matter were investigated. The feasibility of CS on subcortical measurement at lower field strengths such as 1.5T MRI equipped with commonly used 8-channel or 12-channel coils, and different processing software packages have not been intensively investigated.

The objective of this work is to find out whether accelerated CS can be pushed with the 3D-TFE T1W acquisition without compromising its utility on 1.5T MRI equipped with 12-channel head coil. We [illegible] reduction from the routine protocol that is

typically used in ADNI and ENIGMA projects (i.e., conventional parallel imaging with acceleration factor of two). The consistencies of these data sets were observed through three different processing packages including Freesurfer, FSL's FIRST, and volBrain. The volumes of subcortical structures including Caudate, Putamen, Pallidum, Hippocampus, Amygdala, and Accumbens obtained from standard SENSE and CS images were statistically assessed.

Materials And Methods

I. Compressed SENSE Theory

According to Philips's reconstruction engine, unlike standard SENSE technology, CS leverages a balanced variable density incoherent under-sampling acquisition scheme and iterative reconstruction to solve an inverse problem with a sparsity constraint. Specifically, an underlying image (u) are obtained from measured data (m) by minimizing the following convex cost function.

$$\min_{\{u \in C\}} (\beta_1 \|\Psi u\|_1 + \beta_2 \|\Gamma^{\frac{1}{2}} u\|_2^2 + \sum_{c=1}^{N_{coils}} \|F_\Omega S_c u - m_c\|_2^2) \quad (1)$$

$\beta_1, \beta_2 > 0$ are regularization parameters. Ψ is a sparsity transform into wavelet domain. Γ is coarse resolution data from the integrated body coil obtained with the SENSE reference scan. F_Ω is a Fourier transform associated with incoherent under-sampled operator Ω. The s_c is the sensitivity profile for coil element c. In this work, regularization parameters were selected as system default. Note that if operator Ω is uniform under-sampled and $\beta_1 = 0$, equation (1) can be referred to as a standard SENSE reconstruction.

II. Volunteer and MRI data acquisition

Thirty-three healthy volunteers (24 females, 9 males, 21 ± 2 years old) with no history of neurological or psychiatric illness, head trauma with loss of consciousness, cardiovascular disease, and no abnormal findings on the MRIs, were participated. After the procedure was fully explained, written informed consent approved by local Institutional Review Boards (IRB) was obtained from all volunteers prior to MR imaging. All volunteers underwent the 1.5T MRI (Ingenia; Philips, Best, the Netherlands) equipped with 12-channel receive head coil. Imaging protocol consists of the following sequences covering the entire brain: a sagittal 3D turbo field echo (TFE) T1-weighted sequence (176 slices, voxel size: 0.94x0.94x1.00 mm^3, repetition time (TR)/echo time (TE): 7.4/3.4 ms., and flip angle of 7 degrees). This sequence was repeated three times with different acceleration parameters including SENSE-2, SENSE-4, and CS-4, in which their scan times were 6.00, 3.02, and 3.02 minutes, respectively.

III. Data post-processing

All original DICOM images from scanner were converted to the Neuroimaging Informatics Technology Initiative (NIfTI) format using MRIcroGL software (NeuroImaging Tool & Resources Collaboratory, https://www.nitrc.org). The volumes of subcortical brain structures from all volunteers were obtained by the fully automated segmentation-based algorithms in Freesurfer (https://surfer.nmr.mgh.harvard.edu), FMRIB's Integrated Registration and Segmentation Tool (FIRST) of the FMRIB Software Library (FSL) (https://fsl.fmrib.ox.ac.uk/fsl/fslwiki/), and web-based volBrain (http://volbrain.upv.es.). For Freesurfer and FSL's FRIST, the 'recon-all' and 'run_first_all' scripts were implemented using default parameters – running on Intel Core i7 with Ubuntu 20.04 LTS, 64-bit operating system. Besides, signal to noise ratio (SNR) specific individual subcortical structure was computed as mean divided by standard deviation of signal intensities inside the same volume. Subcortical masks were incorporated during SNR calculation.

IV. Statistical analysis

MATLAB (2016b, The Mathworks, Natick, MA) was used for statistical analyses, graph generations, and SNR calculations. SENSE-2 was considered as a gold standard in this study. To compare the agreement between brain structure volumes obtained from SENSE-2, SENSE-4, and CS-4 images, Wilcoxon signed-rank test, Pearson's correlation, and Bland-Altman plot were performed on each pair of data including, SENSE-2 versus SENSE-4 and SENSE-2 versus CS-4, in which $p\text{-value} < 0.05$ indicated statistical significance. The Pearson's correlation coefficient was calculated to measure the correlation between the two techniques. In addition, the standardized mean difference between two techniques was evaluated through the effect size (*ES*). *ES*-scores were interpreted as follow: trivial: $ES < 0.2$, small: $0.2 \leq ES < 0.5$, moderate: $0.5 \leq ES < 0.8$, and large: $ES \geq 0.8$.

Results

I. Visual inspection and SNR assessment

Figure 1 illustrates the pre-processed images that were acquired with different acceleration factors. SENSE-2 images appear substantial quality in all three planes (i.e., sagittal, coronal, and axial) – all structures are clearly visible. In contrast, SENSE-4 images are highly corrupted by noise, particularly at brain stem and cerebellum areas. Fact that these two areas are not well-localized by coil sensitivity, resulting in low SNR and high g-factor amplification. CS-4 enables minimizing ill-posed inverse problem – noise level appears much lower than SENSE-4, but only slightly higher than in SENSE-2, whereas its scan time is reduced half. In comparison with SENSE-2, Fig. 2 demonstrates SNR drops in SENSE-4 for all subcortical structures ($p < 0.01$). As expected, SENSE-2 provides higher SNR values than these values in SENSE-4 and CS-4 for all observed structures. CS-4 was slightly degraded – significant SNR drops were detected only at Pallidum and Amygdala ($p < 0.05$). Two largest SNR drops in SENSE-4 were detected at Pallidum and Accumbens with values of 47.47% and 51.96%, respectively. Meanwhile, the SNR drops in CS-4 were detected at Pallidum and Amygdala with values of 7.34% and 10.55%, respectively.

In Table 1, the results were obtained by Freesurfer. For SENSE-2 versus CS-4, Wilcoxon sign-rank statistic demonstrates that there were no differences of volumes between these two acquisitions for all subcortical structures. These subcortical volumes were in strong correlation indicated by Pearson's correlation coefficients (*r*), in which *r*-values are larger than 0.90. Moreover, their *ES* scores are mostly in trivial to small range with absolute values of 0.07–0.23. The moderate volume difference was only detected at Thalamus, Pallidum, and Amygdala with absolute values of 0.57–0.75. For SENSE-2 versus SENSE-4, there were four subcortical volumes that were significantly different including Thalamus, Pallidum, Amygdala, and Accumbens ($p < 0.05$). Although their correlation coefficients appeared strong with *r*-values of higher than 0.8, the volume differences are somewhat large with absolute scores of higher than 1.5. Only Putamen had strong correlation and trivial volume difference with *r*-value and *ES*-score of 0.99 and 0.01, respectively.

Table 1

Mean and SD of seven subcortical volumes in unit of millimeter cube calculated by using Freesurfer package. Wilcoxon sign-rank test was implemented to assess volume differences in SENSE-4 and CS-4 compared to SENSE-2. *p < 0.05* indicates statistical significance.

Brain Structures ***(n = 33)***	**SENSE-2** **(mm.^{3})**	**SENSE-4** **(mm.^{3})**	**CS-4** **(mm.^{3})**	**SENSE-2 Vs. SENSE-4**	**SENSE-2 vs. CS-4**
	Mean ± SD	***Mean ± SD***	***Mean ± SD***		
Caudate	7155.44 ± 803.34	7071.3 ± 847.1	7142.82 ± 797.54	*p = 0.63* *r = 0.97* *ES = 0.43*	*p = 0.89* *r = 0.97* *ES = 0.07*
Putamen	10420.19 ± 881.5	10420.74 ± 825.47	10465.58 ± 872.34	*p = 0.97* *r = 0.99* *ES < 0.01*	*p = 0.86* *r = 0.97* *ES = − 0.23*
Thalamus	14271.89 ± 1188.74	15828.83 ± 1489.01	14452.88 ± 1243.32	*p < 0.05* *r = 0.98* *es = -3.97*	*p = 0.46* *r = 0.98* *ES = -0.79*
Pallidum	3851.66 ± 379.81	3571.62 ± 327.06	3931.75 ± 391.53	*p < 0.05* *r = 0.87* *ES = 1.52*	*p = 0.31* *r = 0.96* *ES = − 0.75*
Hippocampus	7605.89 ± 625.92	7364.55 ± 593.31	7600.77 ± 614.12	*p = 0.14* *r = 0.97* *ES = 1.77*	*p = 0.93* *r = 0.96* *ES = 0.03*
Amygdala	3082.72 ± 281.16	2643.55 ± 238.18	3030.08 ± 273.41	*p < 0.05* *r = 0.86* *ES = 3.06*	*p = 0.43* *r = 0.94* *ES = 0.57*

Loading [MathJax]/jax/output/CommonHTML/fonts/TeX/fontdata.js andard deviation, CS: compressed SENSE

Brain Structures *(n = 33)*	SENSE-2 ($mm.^3$)	SENSE-4 ($mm.^3$)	CS-4 ($mm.^3$)	SENSE-2 Vs. SENSE-4	SENSE-2 vs. CS-4
	Mean ± SD	*Mean ± SD*	*Mean ± SD*		
Accumbens	1183.98 ± 128.62	985.99 ± 124.71	1174.44 ± 129.78	*p < 0.05* *r = 0.84* *ES = 2.74*	*p = 0.75* *r = 0.94* *ES = 0.22*

ES: effect size, *r*: Pearson's correlation coefficient, *SD*: standard deviation, CS: compressed SENSE

In Table 2, the results were obtained by FSL's FIRST. There was only Amygdala obtained by SENSE-4 has significant different ($p < 0.05$) with moderate correlation ($r = 0.55$) and large volume difference ($ES = -1.29$). Although the other six volumes obtained by SENSE-4 had no statistical significance, the moderate correlation was found at Accumbens ($r = 0.63$). Moreover, large volume differences were also detected at Putamen and Thalamus with absolute *ES*-scores of 1.09 and 0.94, respectively. In contrast, correlation coefficients associated with SENSE-4 versus CS-4 are very high for all subcortical structures ($0.73 < r < 0.98$). In addition, almost *ES*-scores were in the trivial range ($0.03 < ES < 0.2$). Only Amygdala had moderate volume difference with absolute *ES*-score of 0.66.

Table 2

Mean and SD of seven subcortical volumes in unit of millimeter cube calculated by using FSL's FIRST package. Wilcoxon sign-rank test was implemented to assess volume differences in SENSE-4 and CS-4 compared to SENSE-2. *p < 0.05* indicates statistical significance.

Brain Structures (n = 33)	**SENSE-2** ($mm.^3$)	**SENSE-4** ($mm.^3$)	**CS-4** ($mm.^3$)	**SENSE-2 vs. SENSE-4**	**SENSE-2 vs. CS-4**
	Mean ± SD	***Mean ± SD***	***Mean ± SD***		
Caudate	7079.7 ± 672.73	7136.97 ± 679.13	7072.73 ± 699.56	*p = 0.56* *r = 0.86* *ES = -0.15*	*p = 0.92* *r = 0.94* *ES = 0.03*
Putamen	9947.58 ± 710.16	9676.9 ± 7731.11	9970.38 ± 52.05	*p = 0.12* *r = 0.94* *ES = 1.09*	*p = 0.96* *r = 0.95* *ES =-0.08*
Thalamus	14711.21 ± 1018.17	15046.36 ± 1081.03	14747.88 ± 1073.6	*p = 0.18* *r = 0.94* *ES = -0.94*	*p = 0.75* *r = 0.98* *ES =-0.16*
Pallidum	3201.52 ± 306.83	3265.15 ± 332.04	3210.61 ± 269.87	*p = 0.43* *r = 0.82* *ES = -0.33*	*p = 0.91* *r = 0.94* *ES =-0.08*
Hippocampus	7841.21 ± 763.4	7563.33 ± 653.57	7777.27 ± 738.21	*p = 0.08* *r = 0.78* *ES = 0.58*	*p = 0.73* *r = 0.84* *ES = 0.15*
Amygdala	2132.732 ± 99.58	2531.21 ± 348.75	2255.76 ± 371.95	*p < 0.05* *r = 0.55* *ES = -1.29*	*p = 0.12* *r = 0.86* *ES = -0.66*

andard deviation, CS: compressed SENSE

Brain Structures (n = 33)	SENSE-2 ($mm.^3$)	SENSE-4 ($mm.^3$)	CS-4 ($mm.^3$)	SENSE-2 vs. SENSE-4	SENSE-2 vs. CS-4
	Mean ± SD	*Mean ± SD*	*Mean ± SD*		
Accumbens	997.27 ± 145.46	968.79 ± 167.87	974.85 ± 154.66	*p = 0.26* *r = 0.63* *ES = 0.21*	*p = 0.43* *r = 0.73* *ES = 0.20*

ES: effect size, *r*: Pearson's correlation coefficient, *SD*: standard deviation, CS: compressed SENSE

In Table 3, the results were obtained by volBrain. For SENSE-2 versus SENSE-4, there were five among seven subcortical volumes including Putamen, Pallidum, Thalamus, Amygdala, and Accumbens that had significant differences ($p < 0.05$). Moderate and strong correlations were detected at those structures ($0.59 < r < 0.87$), albeit very large volume differences – absolute *ES*-scores were 1.26, 2.53, 3.94, 3.52, and 3.01, respectively. For SENSE-2 versus CS-4, there were no significant differences for all subcortical volumes. Pearson's correlation coefficients and effect size scores were mostly in very strong and trivial ranges, respectively.

Table 3

Mean and SD of seven subcortical volumes in unit of millimeter cube calculated by using volBrain package. Wilcoxon sign-rank test was implemented to assess volume differences in SENSE-4 and CS-4 compared to SENSE-2. *p < 0.05* indicates statistical significance.

Brain Structures ***(n = 33)***	**SENSE-2** **(mm.^{3})**	**SENSE-4** **(mm.^{3})**	**CS-4** **(mm.^{3})**	**SENSE-2 vs. SENSE-4**	**SENSE-2 vs. CS-4**
	Mean ± SD	***Mean ± SD***	***Mean ± SD***		
Caudate	7420.91 ± 870.16	7244.24 ± 800.05	7401.52 ± 840.6	*p = 0.41* *r = 0.95* *ES = 0.66*	*p = 0.88* *r = 0.99* *ES = 0.16*
Putamen	8927.88 ± 760.51	8417.27 ± 765.6	8910.91 ± 752.44	*p < 0.05* *r = 0.86* *ES = 1.26*	*p = 0.91* *r = 0.98* *ES = 0.12*
Thalamus	11687.88 ± 780.19	10568.79 ± 893.7	11745.45 ± 863.63	*p < 0.05* *r = 0.87* *ES = 2.53*	*p = 0.64* *r = 0.97* *ES =-0.25*
Pallidum	2361.52 ± 234.9	1327.88 ± 319.27	2247.27 ± 280.54	*p < 0.05* *r = 0.59* *ES = 3.94*	*p = 0.10* *r = 0.93* *ES = 1.07*
Hippocampus	7573.33 ± 680.37	7352.12 ± 649.45	7610.3 ± 677.65	*p = 0.17* *r = 0.94* *ES = 0.94*	*p = 0.79* *r = 0.99* *ES =-0.55*
Amygdala	1550.91 ± 175.9	1147.58 ± 157.14	1506.97 ± 183.12	*p < 0.05* *r = 0.77* *ES = 3.52*	*p = 0.29* *r = 0.90* *ES = 0.54*

andard deviation, CS: compressed SENSE

Brain Structures *(n = 33)*	SENSE-2 ($mm.^3$)	SENSE-4 ($mm.^3$)	CS-4 ($mm.^3$)	SENSE-2 vs. SENSE-4	SENSE-2 vs. CS-4
	Mean ± SD	*Mean ± SD*	*Mean ± SD*		
Accumbens	652.73 ± 80.28	478.79 ± 82.94	661.52 ± 85.55	*p < 0.05* *r = 0.71* *ES = 3.01*	*p = 0.57* *r = 0.95* *ES =-0.32*

ES: effect size, *r*: Pearson's correlation coefficient, *SD*: standard deviation, CS: compressed SENSE

In addition, one processed data set was randomly picked up for 3D visualization. The Amygdala obtained from SENSE-4 images was found in irregular shape compared to SENSE-2 and CS-4 as highlighted by white circle in Fig. 3. This evidence can support the consistent results in Table 1–3.

III. Bias and limit of agreement between acquisition techniques

Figure 4 and Fig. 5 show Bland-Altman plots for seven subcortical volumes obtained from SENSE-2 versus CS-4 and SENSE-2 versus SENSE-4, respectively. Generally, there should be three plots for each subcortical structure according three post-processing packages. However, one of them that has smallest bias was shown here. For SENSE-2 versus CS-4 (Fig. 4), minimum bias was found at Hippocampus - mean of difference was only − 5.1 mm^3 and limit of agreement (mean ± 1.96 SD) was [-310 300] mm^3. Mean differences and limits of agreements for the other subcortical volumes were less than 44 mm^3 and [-400 470] mm^3, respectively. In contrast, for SENSE-2 versus SENSE-4 (Fig. 5), minimum bias was found at Accumbens - mean of difference was − 28.0 mm^3 and limit of agreement (mean ± 1.96 SD) was [-290 240] mm^3. Mean differences and limits of agreements for the other subcortical volumes were up to -400 mm^3 and [-360 1000] mm^3, respectively.

Discussion

This study evaluated Compressed SENSE for 3D TFE T1-weighted brain imaging sequence with an acceleration factor of four to push 50% time reduction compared to the standard protocol that utilizes a traditional parallel imaging techniques (SENSE-2 or GRAPPA-2). It has been obvious that SENSE-2 and GRAPPA-2 are sufficient and recommended for 3D TFE by ADNI protocol as justified by previous studies [5–6, 17–20]. Some studies used data from ADNI to observe the effect of changing from non-accelerated to accelerated MRI (factor of two) on brain volume measurement. Krueger G. et al [18] found that pairs-of-scans acquired with different accelerations exhibited poor scan–rescan consistency only when using the acceleration factor of five. Manning EN. et al [20] reported that across different sites with the same scanner vendor the effect on K means normalized boundary shift integral when changing from the non-

accelerated to accelerated MRI during follow-up showed minor differences. The variability in sites with Philips scanners appears to be more consistent than with Siemens and GE. Falkovskiy P. et al [29] demonstrated that the four-fold accelerated protocols with either 2D-GRAPPA or CAIPIRINHA introduce systematic biases in the segmentation results of some brain structures compared to the reference ADNI-2 protocol. Ching C. et al [30–31] showed that the estimated atrophy rates from consistent non-accelerated and accelerated acquisitions were very similar, and that they had similar power to track brain changes.

Only few studies have demonstrated an application of compressed sensing MRI on brain volume measurement. In 2019, Mair RW. et al [26] demonstrated that CS-6 with scan time 1.02 minutes can be pushed with 3D-MPRAGE. It should be noted that all scans were performed on 3T MRI equipped with 64-channel head coil. In 2020, Shin DD. et al [27] reported 3T MRI equipped with 32-channel receive coil enabled CS-4.6 for 3D T1W. Three healthy volunteers were recruited. The data sets in two studies above were processed using Freesurfer. Their results showed no major impact on image quality and morphometric measures. Unfortunately, statistical analyses were not performed. In 2020, another study [28] evaluated the image quality, group comparison and cost-effectiveness of different acceleration factors of CS (factors of 3, 4.5 and 6) in healthy controls, multiple sclerosis (MS), and Alzheimer's disease (AD) patients compared to the non-accelerated 3D T1W-TFE sequence on 3T MRI equipped with 32-channel receive coil. They found that signal-to-noise and contrast-to-noise ratios were significantly decreased in all accelerated sequences compared to those of non-accelerated data. CS-6 showed better image quality than SENSE-3 which is consistent with previous studies [32–33]. According to image quality metrics and intraclass correlation coefficients, they concluded that CS-3 is the appropriate acceleration factor for 3D T1W-TFE with well-preserved visual image quality and fewer artifacts for clinical practice.

Unlike previous studies, we implemented CS technique on clinical 1.5T scanner equipped with 12-channel receive coil. Only CS-4 was intensively investigated to confirm whether it is able to replace standard protocol for brain volume measurement. Its SNR values at all brain structures were lower than these values obtained from SENSE-2 data as similar trend as reported in the previous studies [28]. However, we believe that CS-4 could provide other quality matrices related to motion better than SENSE-2 due to shorter scan time which should be suitable for patients who are uncooperative. For volume assessments, no major considerations were found from CS-4 data sets. Its utilities were statically identical to SENSE-2 data sets. For SENSE-4, we found that size of structures and SNR drops were a major relevance, resulting in high variations among post-processing packages. For example, Amygdala and Accumbens have relatively small volume sizes and large SNR drop, resulting in volume inconsistencies among three post-processing packages as demonstrated in Table 1–3 and Fig. 3. In contrast, Volume size of Hippocampus is relatively large (> 7,000 $mm.^3$) and its SNR drop (compared to SENSE-2) was only 9.62%, consequently there is no significant differences across those packages. Note that the large SNR drop at Accumbens may be due to its location - fact that g-factor noise associated with multiple fold-over often occurs at the center of the scanned object. Recently, Morey RA. at al [34] reported that reproducibility of subcortical segmentation relies on the anatomical location, size, and neighboring structures, which are difficult to

differentiate from the target structures. They found that high reproducibility was suggested for Hippocampus rather than Amygdala under Freesurfer software. Thus, parallel imaging with high acceleration factors may cause high variations for small brain structures.

Due to the lack of ground truth, robustness and accuracy among different processing packages were not investigated in this work. Some studies [35–37] showed that the measured brain volumes varied among different segmentation methods. Amygdala and Hippocampus of 147 pediatric populations were measured using manual tracing, Freesurfer, and FSL's FIRST. Up to 50.32% volume difference (manual vs. FSL's FIRST) was detected at left Amygdala. They supported a better consistency between manual segmentation and FreeSurfer than FSL-FIRST [35]. Guo C. at al [36] studied on nine MS patients and reported that SPM-based methods overall produced the most consistent results, while FreeSurfer had less variability in WM volume segmentations across scanners and was less affected by WM lesions. Recently, the volBrain software [37] was developed and tested its reproducibility using 20 subjects from OASIS database (www.oasis-brains.org). It was found to be significantly more reproducible than Freesurfer for putamen while FSL's FIRST was significantly better than volBrain and Freesurfer for the pallidum. However, their performances may also vary among phenotypically different groups.

Some limitations should be further investigations. First, various acceleration factors should be performed to justify the most appropriate one for CS-SENSE. Non-accelerated acquisition should be used as reference instead of SENSE-2 (in case of cooperative volunteers). Second, high number of participants or more types of subjects (e.g., AD, MS, and other diseases) should be included to validate either acquisition methods or post-processing tools. Multi-center reproducible studies with using either same or different receive coil types should be investigated. In addition, various research groups [38–41] demonstrated that the human brain is highly variable among phenotypically different groups (i.e., race) with fundamental genetic and environmental disparities in brain morphology and microstructure (e.g., shape, size and volume). Thus, the image acquisitions may rely on these variations as well.

In conclusion, CS-4 can be pushed with the 3D-TFE T1W acquisition without compromising subcortical volume measurements at 1.5T MRI equipped with 12-channel receive coil. Maximum SNR reduction compared to standard SENSE-2 was 10.55% that was detected at Amygdala. However, such disadvantage was insufficient to compromise the efficacy of Freesurfer, FSL's FIRST, and volBrain software packages.

Declarations

Ethical standards

The measurements on human subjects in this study have been approved by the local ethics committee and have therefore been performed in accordance with the ethical standards laid down in the Declaration of Helsinki. All involved participants have given their informed consent before recruitment in the study.

Conflict of interest

The authors have no conflict of interest.

Acknowledgement

This work was financially supported by Faculty of Associated Medical Sciences, Chiang Mai University. We thank Philips (Thailand) Ltd., and Philips Healthcare, Asia Pacific for providing Compressed SENSE technique. We thank Laohawee N., Manonai N., Porploy J., and Yingmeesakul S. for data collecting.

References

1. Giedd JN, Blumenthal J, Jeffries NO, Castellanos FX, Liu H, Zijdenbos A et al (1999) Brain development during childhood and adolescence: a longitudinal MRI study. Nat Neurosci 2:861–863
2. Ashburner J, Friston KJ (2000) Voxel-based morphometry - the methods. Neuroimage 11:805–821
3. Azevedo CJ, Cen SY, Khadka S, Liu S, Kornak J, Shi Y et al (2018) Thalamic atrophy in multiple sclerosis: A magnetic resonance imaging marker of neurodegeneration throughout disease. Ann Neurol 83(2):223–234
4. Pini L, Pievani M, Bocchetta M, Altomare D, Bosco P, Cavedo E et al (2016) Brain atrophy in Alzheimer's Disease and aging. Ageing Res Rev 30:25–48
5. Jack CR Jr, Bernstein MA, Fox NC, Thompson P, Alexander G, Harvey D et al. The Alzheimer's Disease Neuroimaging Initiative (ADNI): MRI methods. J Magn Reson Imaging 27:685–691
6. Petersen RC, Aisen PS, Beckett LA et al (2010) Alzheimer's Disease Neuroimaging Initiative (ADNI): clinical characterization. Neurology 74(3):201–209
7. van Erp TG, Hibar DP, Rasmussen JM et al (2016) Subcortical brain volume abnormalities in 2028 individuals with schizophrenia and 2540 healthy controls via the ENIGMA consortium. Mol Psychiatry 21(4):547–553
8. van Erp TG, Greve DN, Rasmussen J et al (2014) A multi-scanner study of subcortical brain volume abnormalities in schizophrenia. Psychiatry Res 222(1–2):10–16
9. Jovicich J, Czanner S, Han X et al (2009) MRI-derived measurements of human subcortical, ventricular and intracranial brain volumes: Reliability effects of scan sessions, acquisition sequences, data analyses, scanner upgrade, scanner vendors and field strengths. Neuroimage 46(1):177–192
10. Godenschweger F, Kägebein U, Stucht D, Yarach U, Sciarra A, Yakupov R et al (2016) Motion correction in MRI of the brain. Physics in medicine biology 61(5):R32–R56
11. Havsteen I, Ohlhues A, Madsen KH, Nybing JD, Christensen H, Christensen A (2017) Are Movement Artifacts in Magnetic Resonance Imaging a Real Problem? - A Narrative Review. Frontiers in neurology 8,232

12. Pruessmann KP, Weiger M, Scheidegger MB, Boesiger P (1999) SENSE: sensitivity encoding for fast MRI. Magn Reson Med 42(5):952–962
13. Griswold MA, Jakob PM, Heidemann RM, Nittka M, Jellus V, Wang J et al (2002) Generalized autocalibrating partially parallel acquisitions (GRAPPA). Magn Reson Med 47(6):1202–1210
14. Sodickson DK, Griswold MA, Jakob PM (1999) SMASH imaging. Magn Reson Imaging Clin N Am 7(2):237–254
15. Hamilton J, Franson D, Seiberlich N (2017) Recent advances in parallel imaging for MRI. Progress Nucl Magn Reson Spectrosc 101:71–95
16. Lin FH, Huang T, Chen NK, Wang FN, Stufflebeam SM, Belliveau JW et al (2005) Functional MRI using regularized parallel imaging acquisition. Magnetic resonance in medicine 54(2):343–353
17. Leung KK, Malone IM, Ourselin S et al (2015) Effects of changing from non-accelerated to accelerated MRI for follow-up in brain atrophy measurement. Neuroimage 107:46–53
18. Krueger G, Granziera C, Jack CR Jr et al (2012) Effects of MRI scan acceleration on brain volume measurement consistency. J Magn Reson Imaging 36(5):1234–1240
19. Maclaren J, Han Z, Vos SB, Fischbein N, Bammer R (2014) Reliability of brain volume measurements: a test-retest dataset. Sci Data 1:140037
20. Manning EN, Leung KK, Nicholas JM et al (2017) A Comparison of Accelerated and Non-accelerated MRI Scans for Brain Volume and Boundary Shift Integral Measures of Volume Change: Evidence from the ADNI Dataset. Neuroinformatics 15(2):215–226
21. Lustig M, Donoho DL, Santos JM, Pauly JM (2008) Compressed Sensing MRI. IEEE Signal Process Mag 25(2):72–82
22. Lustig M, Donoho D, Pauly JM (2007) Sparse MRI: The application of compressed sensing for rapid MR imaging. Magn Reson Med 58(6):1182–1195
23. Otazo R, Kim D, Axel L, Sodickson DK (2010) Combination of compressed sensing and parallel imaging for highly accelerated first-pass cardiac perfusion MRI. Magn Reson Med 64(3):767–776
24. Jaspan ON, Fleysher R, Lipton ML (2015) Compressed sensing MRI: a review of the clinical literature. Br J Radiol 88(1056):20150487
25. Smith DS, Li X, Abramson RG, Quarles CC, Yankeelov TE, Welch EB (2013) Potential of compressed sensing in quantitative MR imaging of cancer. Cancer Imaging 13(4):633–644
26. Mair RW, Hanford LC, Mussard E, Hilbert T, Kober T, Buckner RL (2019) Towards 1 min brain morphometry - evaluating compressed-sensing MPRAGE. In Proc. Int. Soc. Magn. Reson. Med. p. 2978
27. Shin DD, Rettmann D, Takei N, Banerjee S (2020) Compressed Sensed MPRAGE with Parallel Imaging: Image Quality Metrics and Morphometry Study at 3T. In Proc. Int. Soc. Magn. Reson. Med. p. 1747
28. Duan Y, Zhang J, Zhuo Z, Ding J, Ju R, Wang J et al Accelerating Brain 3D T1-Weighted Turbo Field Echo MRI Using Compressed Sensing-Sensitivity Encoding (CS-SENSE). Eur J Radiol 131:109255

29. Falkovskiy P, Brenner D, Feiweier T et al (2016) Comparison of accelerated T1-weighted whole-brain structural-imaging protocols. Neuroimage 124:157–167
30. Ching CRK, Hua X, Hibar DP, Ward CP, Gunter JL, Bernstein MA et al (2012) the Alzheimers Disease Neuroimaging Initiative. P. M. T. MRI scan acceleration and power to track brain change. MICCAI NIBAD
31. Ching CR, Hua X, Hibar DP, Ward CP, Gunter JL, Bernstein MA et al (2015) Does MRI scan acceleration affect power to track brain change? Neurobiol Aging 1:167–177
32. Sartoretti T, Sartoretti E, van Smoorenburg L, Schwenk Á, Mannil M, Graf N et al (2020) Spiral 3-Dimensional T1-Weighted Turbo Field Echo: Increased Speed for Magnetization-Prepared Gradient Echo Brain Magnetic Resonance Imaging. Invest Radiol 55(12):775–784
33. Sartoretti E, Sartoretti T, Binkert C, Najafi A, Schwenk Á, Hinnen M et al (2019) Reduction of procedure times in routine clinical practice with Compressed SENSE magnetic resonance imaging technique. PloS one 14(4):e0214887
34. Morey RA, Petty CM et al (2009) A comparison of automated segmentation and manual tracing for quantifying hippocampal and amygdala volumes. NeuroImage 45(3):855–866
35. Schoemaker D, Buss C, Head K et al (2016) Hippocampus and amygdala volumes from magnetic resonance images in children: Assessing accuracy of FreeSurfer and FSL against manual segmentation. NeuroImage 129:1–14
36. Guo C, Ferreira D, Fink K, Westman E, Granberg T (2019) Repeatability and reproducibility of FreeSurfer, FSL-SIENAX and SPM brain volumetric measurements and the effect of lesion filling in multiple sclerosis. Eur Radiol 29(3):1355–1364
37. Manjón JV, Coupé P (2016) volBrain: An Online MRI Brain Volumetry System. Front Neuroinform 27:10–30
38. Liang P, Shi L, Chen N et al (2015) Construction of brain atlases based on a multi-center MRI dataset of 2020 Chinese adults. Sci Rep 5:18216
39. Tang Y, Hojatkashani C, Dinov ID, Sun B, Fan L, Lin X et al (2010) The construction of a Chinese MRI brain atlas: a morphometric comparison study between Chinese and Caucasian cohorts. Neuroimage 51:33–41
40. Bai J, Abdul-Rahman MF, Rifkin-Graboi A, Chong YS, Kwek K, Saw SM et al (2012) Population differences in brain morphology and microstructure among Chinese, Malay and Indian neonates. PLoS One 7:e47816
41. Takahashi R, Ishii K, Kakigi T, Yokoyama K (2011) Gender and age differences in normal adult human brain: voxel-based morphometric study. Hum Brain Mapp 32:1050–1058

Figures

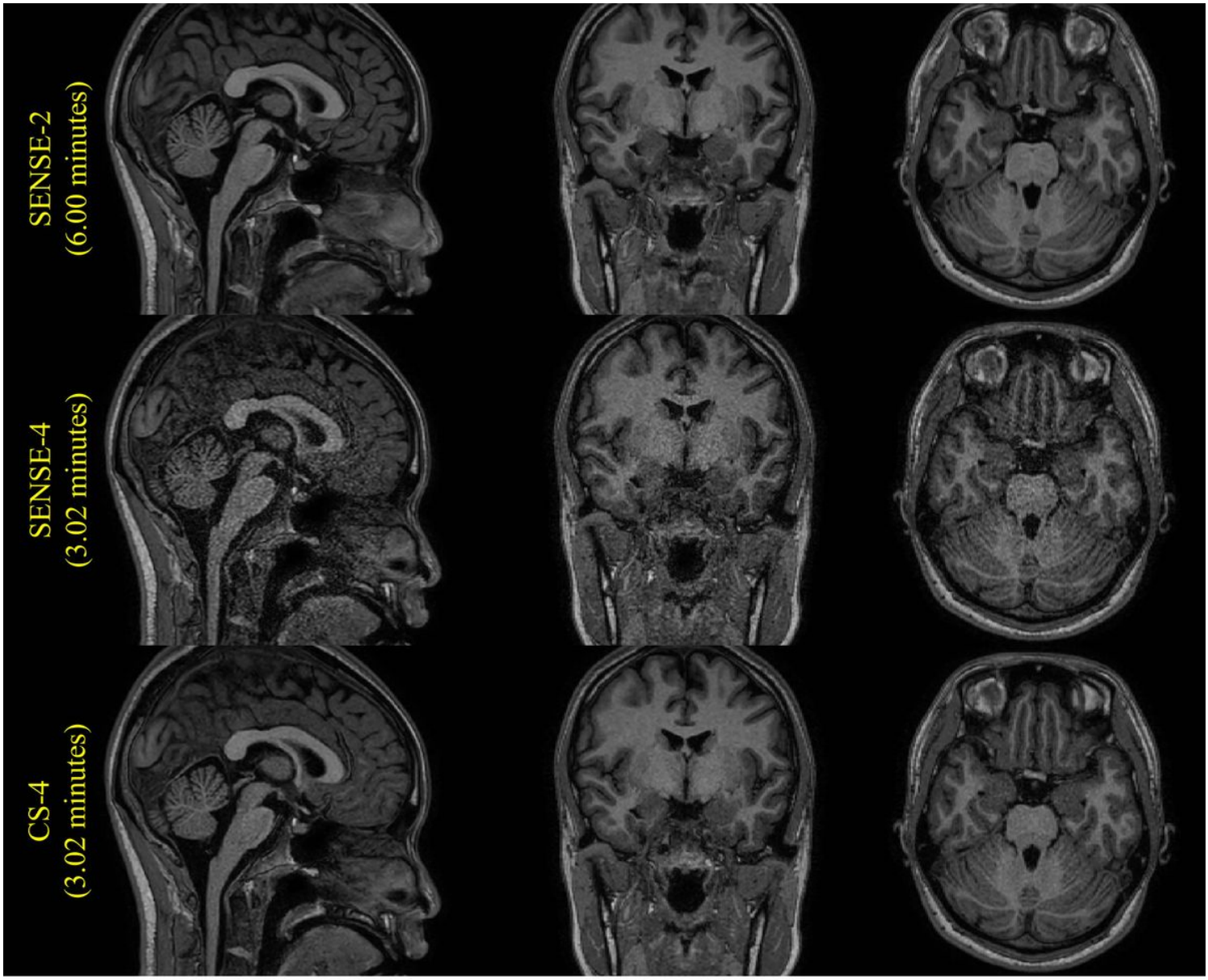

Figure 1

All example images were acquired from the same volunteer with three different acquisition techniques: (top row) SENSE with acceleration factor of two, scan time 6.00 minutes, (middle row) SENSE with acceleration factor of four, scan time 3.02 minutes, and (bottom row) Compressed SENSE with acceleration factor of four, scan time 3.02 minutes.

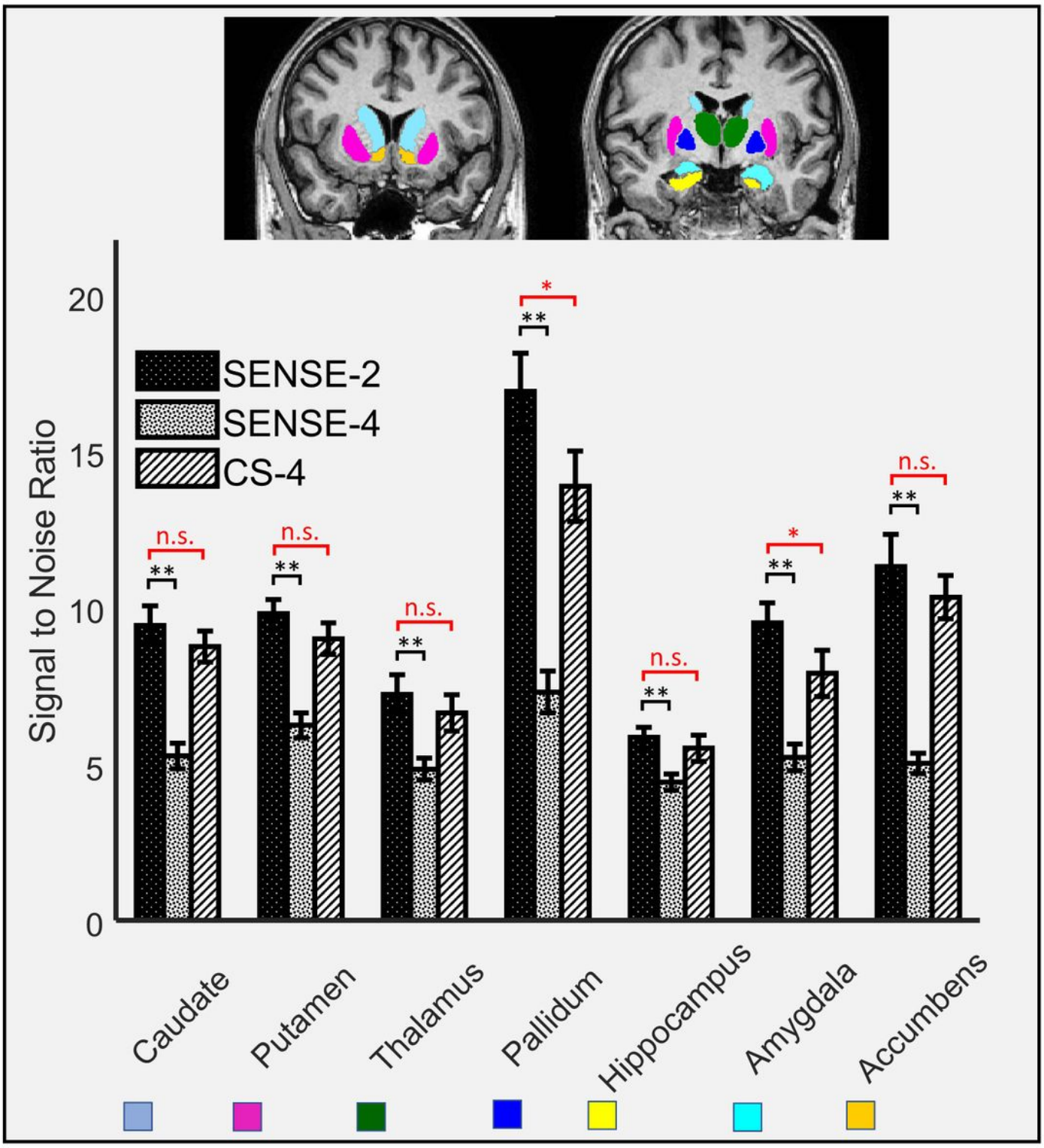

Figure 2

Signal to noise ratio (SNR) was calculated for all seven individual subcortical volumes of thirty-three volunteers. SNR was computed as mean divided by standard deviation of signal intensities inside the same volume, in which subcortical masks were incorporated during SNR calculation. The different colors overlaid on the coronal plane of brain images illustrate seven subcortical structures. Wilcoxon sign-rank

E-4 and CS-4 compared to SENSE-2. “*” and “**”

indicate statistical significance with p<0.05 and p<0.01, respectively. n.s. indicates no statistical significance.

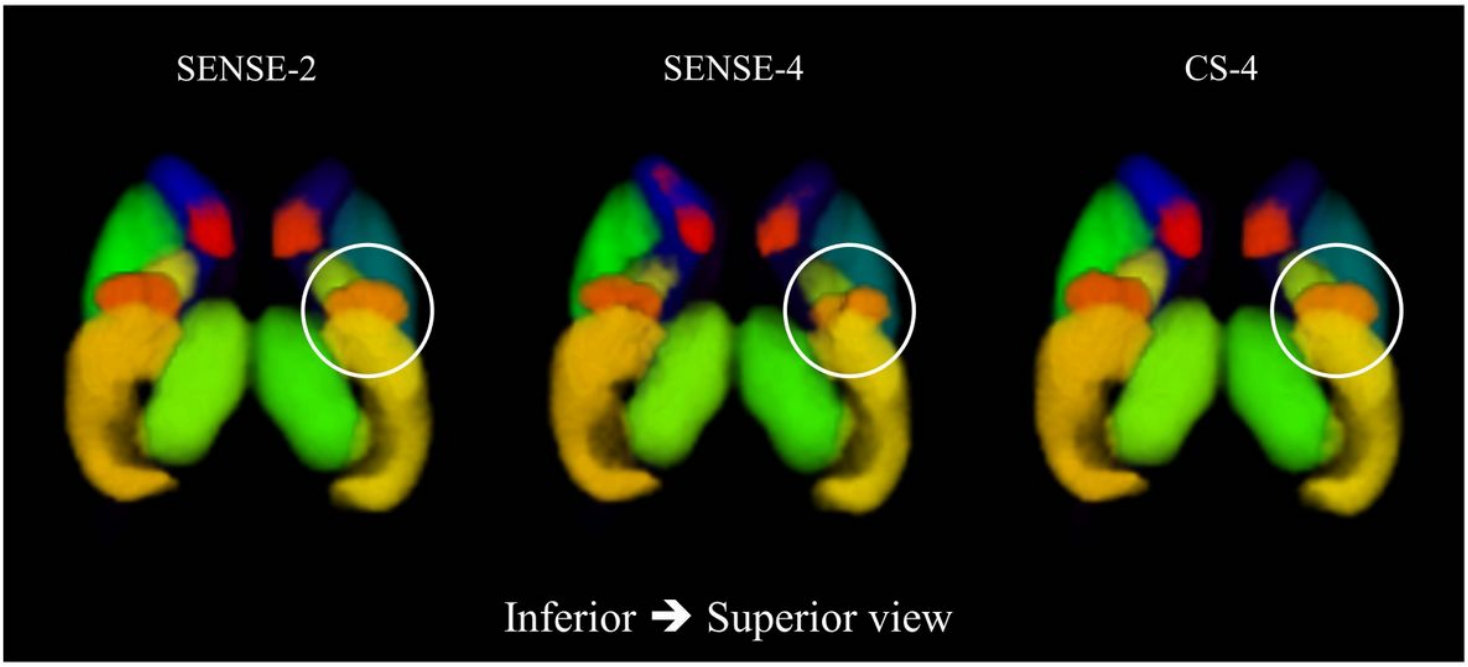

Figure 3

Surface rendering of an MR image showing subcortical structures. White circle at SENSE-4 highlights the irregular shape of Amygdala (orange color).

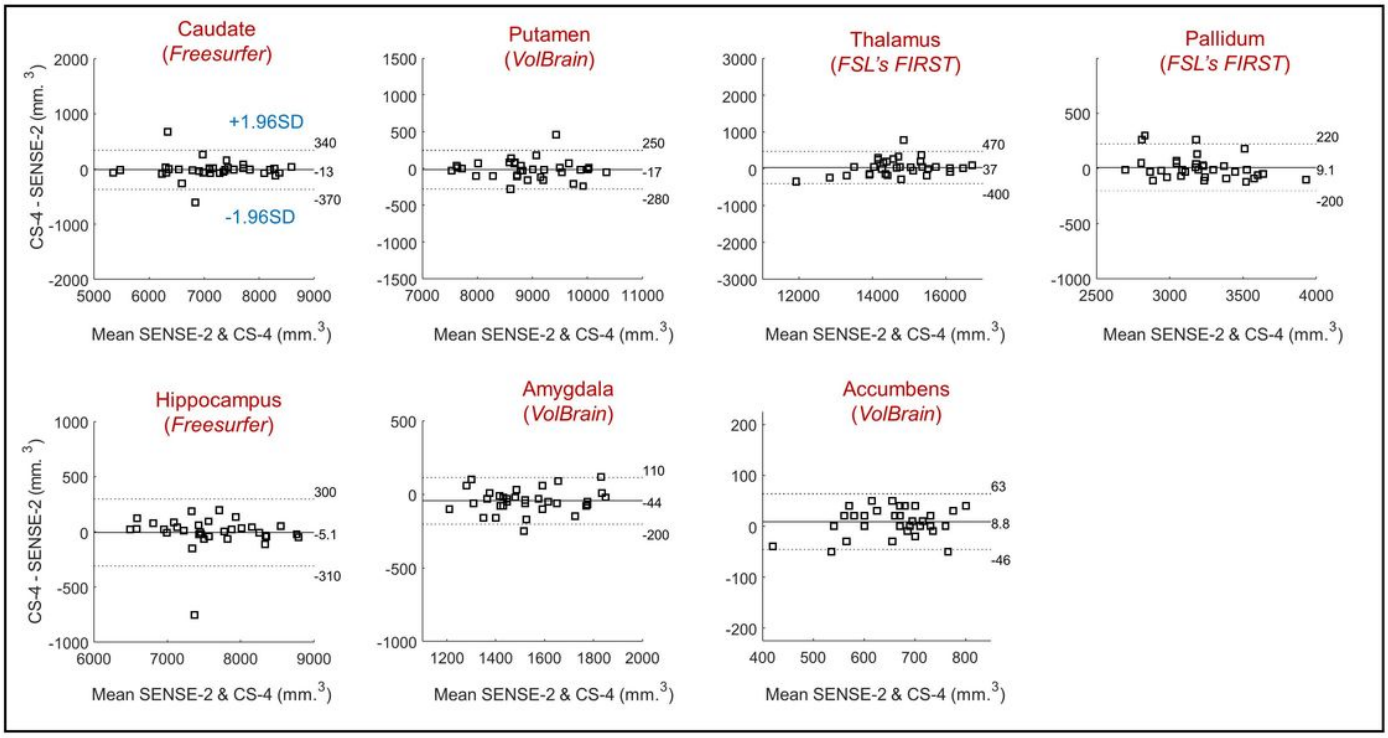

Figure 4

Bland-Altman plots at SENSE-2 and CS-4 for seven individual subcortical volumes obtained by three different software packages. X-axis: mean brain volume measurement at SENSE-2 and CS-4. Y-axis: difference (in mm.3) in brain volume measurement between SENSE-2 and CS-4. The mean, lower (-1.96 SD) and upper (+1.96 SD) limits of agreement are shown. A negative difference on the y-axis is seen when brain volume measurements at CS-4 were larger than at SENSE-2. SD: standard deviation, CS: compressed SENSE.

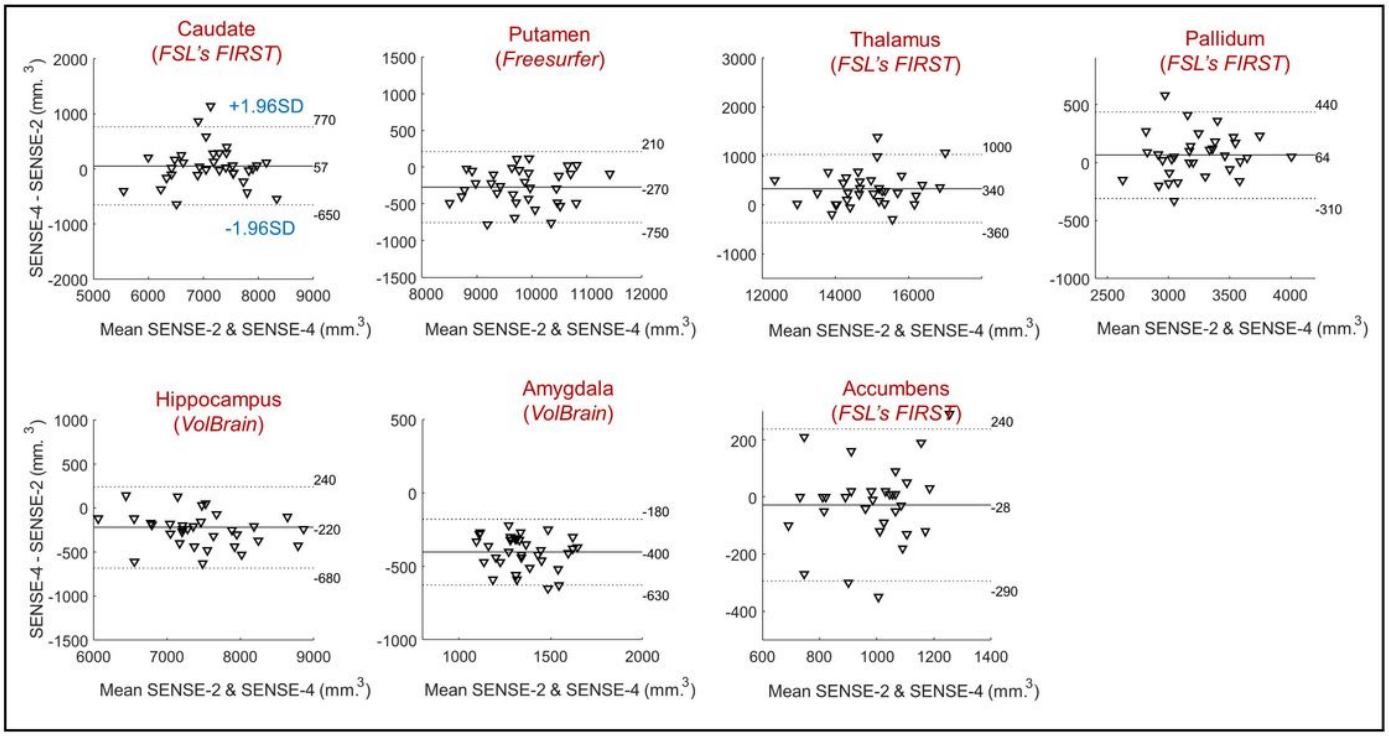

Figure 5

Bland-Altman plots at SENSE-2 and SENSE-4 for seven individual subcortical volumes obtained by three different software packages. X-axis: mean brain volume measurement at SENSE-2 and SENSE-4. Y-axis: difference (in mm.3) in brain volume measurement between SENSE-2 and SENSE-4. The mean, lower (-1.96 SD) and upper (+1.96 SD) limits of agreement are shown. A negative difference on the y-axis is seen when brain volume measurements at SENSE-4 were larger than at SENSE-2. SD: standard deviation, CS: compressed SENSE.